



1 **Coarse particulate matter air quality in East Asia:**  
2 **implications for fine particulate nitrate**

3 Shixian Zhai<sup>1,\*</sup>, Daniel J. Jacob<sup>1</sup>, Drew C. Pendergrass<sup>1</sup>, Nadia K. Colombi<sup>2</sup>, Viral Shah<sup>1</sup>,  
4 Laura Hyesung Yang<sup>1</sup>, Qiang Zhang<sup>3</sup>, Shuxiao Wang<sup>4</sup>, Hwajin Kim<sup>5</sup>, Yele Sun<sup>6</sup>, Jin-Soo  
5 Choi<sup>7</sup>, Jin-Soo Park<sup>7</sup>, Gan Luo<sup>8</sup>, Fangqun Yu<sup>8</sup>, Jung-Hun Woo<sup>9</sup>, Younha Kim<sup>10</sup>, Jack E.  
6 Dibb<sup>11</sup>, Taehyoung Lee<sup>12</sup>, Jin-Seok Han<sup>13</sup>, Bruce E. Anderson<sup>14</sup>, Ke Li<sup>15</sup>, Hong Liao<sup>15</sup>  
7

8 <sup>1</sup> John A. Paulson School of Engineering and Applied Sciences, Harvard University, Cambridge, MA 02138

9 <sup>2</sup> Department of Earth and Planetary Science, Harvard University, Cambridge, MA 02138, USA

10 <sup>3</sup> Department of Earth System Science, Tsinghua University, Beijing 100084, China

11 <sup>4</sup> State Key Joint Laboratory of Environmental Simulation and Pollution Control, School of Environment,  
12 Tsinghua University, Beijing 100084, China

13 <sup>5</sup> Department of Environmental Health Sciences, Graduate School of Public Health, Seoul National  
14 University, Seoul 08826, South Korea

15 <sup>6</sup> State Key Laboratory of Atmospheric Boundary Layer Physics and Atmospheric Chemistry, Institute of  
16 Atmospheric Physics, Chinese Academy of Sciences, Beijing 100029, China

17 <sup>7</sup> Air Quality Research Division, National Institute of Environmental Research, Incheon 22689, Republic of  
18 Korea

19 <sup>8</sup> Atmospheric Sciences Research Center, University at Albany, Albany, NY 12226, USA

20 <sup>9</sup> Department of Civil and Environmental Engineering, Konkuk University, Seoul 05029, South Korea

21 <sup>10</sup> International Institute for Applied Systems Analysis (IIASA), Laxenburg 2361, Austria

22 <sup>11</sup> Institute for the Study of Earth, Oceans, and Space, University of New Hampshire, Durham, NH 03824

23 <sup>12</sup> Department of Environmental Science, Hankuk University of Foreign Studies, Yongin 449791, South  
24 Korea

25 <sup>13</sup> Department of Environmental and Energy Engineering, Anyang University, Anyang 14028, South Korea

26 <sup>14</sup> NASA Langley Research Center, Hampton, VA 23681, USA

27 <sup>15</sup> Jiangsu Key Laboratory of Atmospheric Environment Monitoring and Pollution Control, Collaborative  
28 Innovation Center of Atmospheric Environment and Equipment Technology, School of Environmental  
29 Science and Engineering, Nanjing University of Information Science and Technology, Nanjing 210044,  
30 China

31 *Correspondence to:* Shixian Zhai (zhaisx@g.harvard.edu)

32



33 **Abstract.** Air quality network data in China and South Korea show very high year-round mass  
34 concentrations of coarse particulate matter (PM), as inferred by difference between  $PM_{10}$  and  $PM_{2.5}$ . Coarse  
35 PM concentrations in 2015 averaged  $52 \mu\text{g m}^{-3}$  in the North China Plain (NCP) and  $23 \mu\text{g m}^{-3}$  in the Seoul  
36 Metropolitan Area (SMA), contributing nearly half of  $PM_{10}$ . Strong daily correlations between coarse PM  
37 and carbon monoxide imply a dominant source from anthropogenic fugitive dust. Coarse PM  
38 concentrations in the NCP and the SMA decreased by 21% from 2015 to 2019 and further dropped abruptly  
39 in 2020 due to COVID-19 reductions in construction and vehicle traffic. Anthropogenic coarse PM is  
40 generally not included in air quality models but scavenges nitric acid to suppress the formation of fine  
41 particulate nitrate, a major contributor to  $PM_{2.5}$  pollution. GEOS-Chem model simulation of surface and  
42 aircraft observations from the KORUS-AQ campaign over the SMA in May-June 2016 shows that  
43 consideration of anthropogenic coarse PM largely resolves the previous model overestimate of fine  
44 particulate nitrate. The effect is smaller in the NCP which has a larger excess of ammonia. Model  
45 sensitivity simulations show that decreasing anthropogenic coarse PM over 2015-2019 directly increases  
46  $PM_{2.5}$  nitrate in summer, offsetting half the effect of other emission controls, while in winter it increases the  
47 sensitivity of  $PM_{2.5}$  nitrate to ammonia and sulfur dioxide emissions. Decreasing coarse PM helps to  
48 explain the flat wintertime  $PM_{2.5}$  nitrate trends observed in the NCP and the SMA despite decreases in  
49 nitrogen oxides and ammonia emissions. The continuing decrease of coarse PM from abating fugitive dust  
50 pollution will require more stringent nitrogen oxides and ammonia emission controls to successfully  
51 decrease  $PM_{2.5}$  nitrate.

## 52 1. Introduction

53 Coarse particulate matter (coarse PM; particulate matter between  $2.5 \mu\text{m}$  and  $10 \mu\text{m}$  aerodynamic diameter)  
54 is a severe air pollution problem in East Asia, contributing a particle mass comparable to fine particulate  
55 matter ( $PM_{2.5}$ ) and thus about half of  $PM_{10}$  (Chen et al., 2019; Lee et al., 2015; Qiu et al., 2014; Wang et al.,  
56 2018a). It is mainly fugitive mineral dust, with contributions from both natural desert dust and human  
57 activity including on-road traffic, construction, and agriculture (Wu et al., 2016; Zhao et al., 2017; Liu et  
58 al., 2021; Kutra, 2020). Atmospheric chemistry models used in air quality applications generally do not  
59 include anthropogenic fugitive dust, due to the lack of available emission inventories except for a few  
60 urban areas (Li et al., 2021a; Li et al., 2021b; Li et al., 2021c). Aside from its direct interest as an air  
61 pollutant, coarse PM can suppress  $PM_{2.5}$  by heterogeneously taking up acids ( $\text{HNO}_3$ ,  $\text{SO}_2$ , and  $\text{H}_2\text{SO}_4$ ) that  
62 would otherwise lead to  $PM_{2.5}$  formation. This uptake has been observed for natural dust events (Wang et  
63 al., 2017; Heim et al., 2020; Wang et al., 2018b; Park et al., 2004; Stone et al., 2011), but the more  
64 ubiquitous effect from anthropogenic dust has received little study (Kakavas and Pandis, 2021; Hodzic et  
65 al., 2006). With increasingly stringent control measures to decrease fugitive dust air pollution in East Asia  
66 (Chinese State Council, 2019; Noh et al., 2018; Wu et al., 2016; Xing et al., 2018), it is important to better  
67 understand the impact on  $PM_{2.5}$  air quality.



68 A specific issue is the effect of anthropogenic dust on  $PM_{2.5}$  nitrate. Nitrate is a major component of  
69  $PM_{2.5}$  in urban regions of East Asia including the North China Plain (NCP) (Li et al., 2019; Zhai et al.,  
70 2021a) and the Seoul Metropolitan Area (SMA) (Jeong et al., 2022; Kim et al., 2020), and it can dominate  
71 haze pollution events over both regions (Fu et al., 2020; Li et al., 2018; Xu et al., 2019; Kim et al., 2017;  
72 Kim et al., 2020).  $PM_{2.5}$  nitrate over North China in winter has not decreased in recent years despite  
73 reductions in emissions of the precursor nitrogen oxides ( $NO_x \equiv NO + NO_2$ ) (Zhai et al., 2021a; Fu et al.,  
74 2020) from fossil fuel combustion. This has been attributed to limitation by ammonia ( $NH_3$ ) emissions,  
75 since  $PM_{2.5}$  nitrate is mainly present as ammonium nitrate (Zhai et al., 2021a). Decreasing coarse PM  
76 emissions is another possible explanation as it would allow more  $HNO_3$  to be available for  $PM_{2.5}$  nitrate  
77 formation, and it could also shift  $PM_{2.5}$  nitrate formation to be more  $NH_3$ -limited. Better understanding this  
78 sensitivity of  $PM_{2.5}$  nitrate to coarse PM is of crucial importance because of recent efforts by the Chinese  
79 government to decrease  $NH_3$  emissions (Liao et al., 2022), which are mainly from agriculture with  
80 additional urban contributions from vehicle, industrial, and waste disposal sources (Mgelwa et al., 2022).

81 In this work, we show that coarse PM over the NCP and the SMA is mainly anthropogenic and decreased  
82 by 21% during the 2015–2019 period. We find that accounting for this anthropogenic coarse PM in the  
83 GEOS-Chem atmospheric chemistry model greatly improves the ability of the model to simulate  $PM_{2.5}$   
84 nitrate during the KORUS-AQ aircraft campaign over Korea where previous GEOS-Chem simulations  
85 found a large overestimate (Travis et al., 2022; Zhai et al., 2021b). From there we examine the implications  
86 for the effects of emission controls on long-term trends of  $PM_{2.5}$  nitrate in China and South Korea.

## 87 2. Coarse PM in China and South Korea

88 Figure 1 shows the annual mean concentrations of coarse PM in 2015, 2019, and 2020 measured at air  
89 quality networks in China and South Korea as the  $PM_{10} - PM_{2.5}$  difference. Data for China are from the  
90 Ministry of Ecology and Environment (MEE) network (<http://www.quotsoft.net/air/>) and data for South  
91 Korea are from the AirKorea network (<https://www.airkorea.or.kr>). We remove spurious data when  $PM_{2.5}$  is  
92 higher than  $PM_{10}$ , which account for 1.7% and 0.2% of the dataset respectively in China and South Korea.

93 We see from Fig. 1 that coarse PM concentrations in China and South Korea are highest in the NCP and  
94 the SMA, respectively, indicating a dominant urban anthropogenic origin. Coarse PM in year 2015  
95 averaged  $52 \mu g m^{-3}$  in the NCP and  $23 \mu g m^{-3}$  in the SMA, contributing nearly half of total  $PM_{10}$  ( $120 \mu g m^{-3}$   
96 in the NCP and  $50 \mu g m^{-3}$  in the SMA). National air quality standards for annual mean  $PM_{10}$  are  $70 \mu g m^{-3}$   
97 in China (urban) and  $50 \mu g m^{-3}$  in South Korea, well above the World Health Organization (WHO)  
98 recommended annual standard of  $15 \mu g m^{-3}$ . Coarse PM decreased by 21% in both the NCP and the SMA  
99 from 2015 to 2019, reflecting emission controls on fugitive dust (Council, 2013, 2018; Noh et al., 2018;  
100 Wu et al., 2016), and further decreased strongly in 2020 because of COVID-19 restrictions on traffic and



101 construction. The COVID-19 impact is evident in China by comparing concentrations before and after the  
102 sharp January 24, 2020 lockdown (Fig. 2).

103 Figure 3 shows further evidence of the dominant anthropogenic contribution to coarse PM as the daily  
104 correlation with carbon monoxide (CO) in 2015. CO is emitted by incomplete combustion and is a tracer of  
105 urban influence. We find strong correlations between coarse PM and CO with consistent slopes except in  
106 spring, which features high coarse PM outliers attributable to desert dust events (Heim et al., 2020; Shao  
107 and Dong, 2006). Similar correlations to 2015 are found in other years (Fig. S1). The desert dust events  
108 drive the seasonal maximum of coarse PM in Fig. 1h.

### 109 **3. Effect of anthropogenic coarse PM on fine particulate nitrate during KORUS-AQ**

110 We simulated the effect of anthropogenic coarse PM on  $PM_{2.5}$  nitrate using the GEOS-Chem model and  
111 evaluated the model with observations from the KORUS-AQ aircraft campaign over South Korea in May-  
112 June 2016 (Crawford et al., 2021). KORUS-AQ offers a unique data set of detailed aerosol and gas-phase  
113 composition over East Asia. Previous GEOS-Chem simulations showed a large overestimate of fine  
114 particulate nitrate and a large underestimate of coarse PM (Travis et al., 2022; Zhai et al., 2021b).  
115 Particulate nitrate concentrations were measured during KORUS-AQ at the Korea Institute of Science and  
116 Technology (KIST) surface site and on the aircraft by Aerosol Mass Spectrometers (AMS) with size cut of  
117  $1 \mu m$  diameter ( $PM_1$  nitrate) (Kim et al., 2017; Kim et al., 2018), and also on the aircraft by the Soluble  
118 Acidic Gases and Aerosol (SAGA) instrument with size cut of  $4 \mu m$  diameter ( $PM_4$  nitrate) (Dibb et al.,  
119 2003; Mcnaughton et al., 2007). Additional measurements on the aircraft included  $HNO_3$  concentrations  
120 with a Chemical Ionization Time of Flight Mass Spectrometer (CIT-ToF-CIMS), and aerosol size  
121 distributions including coarse PM with a DMT CPSPD Probe. We focus on the observations over the SMA  
122 and exclude observations from two process-directed flights (RF7 and RF8) and the Daesan power plant  
123 plume following Park et al. (2021).

124 We use GEOS-Chem version 13.0.2 (<https://zenodo.org/record/4681204>) in a nested-grid simulation  
125 over East Asia ( $100 - 150^\circ E$ ,  $20 - 50^\circ N$ ) with a horizontal resolution of  $0.5^\circ \times 0.625^\circ$ . The model simulates  
126 detailed oxidant-aerosol chemistry relevant to  $PM_{2.5}$  nitrate formation (Zhai et al., 2021a) and is driven by  
127 meteorological data from the NASA Modern-Era Retrospective Analysis for Research and Applications,  
128 Version 2 (MERRA-2). Dry deposition of gases and particles follows a standard resistance-in-series  
129 scheme (Wesely, 1989). Wet deposition of gases and particles includes contributions from rainout,  
130 washout, and scavenging in convective updrafts (Liu et al., 2001; Luo et al., 2019). The model includes  
131 reactive uptake of  $HNO_3$  on dust limited by dust alkalinity and mass transfer (Fairlie et al., 2010), assuming  
132 7.1 %  $Ca^{2+}$  and 1.1%  $Mg^{2+}$  as carbonates per mass in emitted dust (Shah et al., 2020a; Tang and Han, 2017;  
133 Zhang et al., 2014). The relative humidity (RH)-dependent reactive uptake coefficient ( $\gamma$ ) of  $HNO_3$  is based  
134 on laboratory studies (Liu et al., 2008; Huynh and Mcneill, 2020) and observations during natural dust



135 events in Beijing (Tian et al., 2021; Wang et al., 2017), and increases from 0.06 to 0.21 as RH increases  
136 from 40% to 80%. Monthly anthropogenic emissions for China are from the Multi-resolution Emission  
137 Inventory for China (MEIC) (Zheng et al., 2018; Zheng et al., 2021a; Zheng et al., 2021b), and emissions  
138 for other Asian countries including South Korea are from the KORUSv5 inventory (Woo et al., 2020). Fine  
139 anthropogenic mineral dust emissions from combustion and industrial sources (ash) are derived from the  
140 MEIC and KORUSv5 inventories as the residual of anthropogenic primary  $PM_{2.5}$  emissions after excluding  
141 primary organic aerosol, black carbon, and primary sulfate (Philip et al., 2017).

142 We compare the results from the standard model as described above to a simulation where we add  
143 anthropogenic coarse PM by using 24-hour average coarse PM observations from the air quality networks  
144 (Fig. 1) as boundary conditions at the lowest model level. For this purpose, we linearly interpolate the daily  
145 network data to the GEOS-Chem model grid and apply them to the coarse dust GEOS-Chem model  
146 component with an effective diameter of 4.8  $\mu m$ . Anthropogenic coarse PM is assumed to be mainly  
147 fugitive dust with the same alkalinity properties as natural dust (Zhang et al., 2014; Tang and Han, 2017).

148 Figure 4 compares GEOS-Chem to the KORUS-AQ observations including median diurnal  $PM_1$  nitrate  
149 at the KIST site and median aircraft vertical profiles over the SMA. The model is sampled along the aircraft  
150 flight tracks at the times of the observations, all in daytime.  $PM_1$  nitrate in the observations was mainly  
151 associated with ammonium (Fig. S2). Here we take ammonium nitrate in the model for comparison to  $PM_1$   
152 observations, and size-resolved dust nitrate for comparison to  $PM_{1.4}$  observations. GEOS-Chem results are  
153 shown both for the standard model (not including anthropogenic coarse PM) and with the addition of  
154 anthropogenic coarse PM. In both simulations, we adjusted the diurnal variation of  $NH_3$  emission to match  
155 the  $NH_3$  observations made at the Olympic Park site, 7 km southeast of KIST (Fig. S3).

156 The standard GEOS-Chem simulation overestimates daytime  $PM_1$  nitrate (aircraft and surface) by about  
157 a factor of two while underestimating  $PM_{1.4}$  nitrate by about a factor of two (Fig. 4a, b, and c). Coarse PM  
158 in the standard simulation (from natural dust and sea salt) is near zero, considerably underestimating  
159 observations (Fig. 4d). Adding anthropogenic coarse PM to the model corrects this bias and further corrects  
160 the  $PM_1$  and  $PM_{1.4}$  nitrate biases. We find that anthropogenic coarse PM takes up  $HNO_3$  three times faster  
161 than dry deposition and that this uptake is not limited by alkalinity (only 60% of the dust alkalinity in  
162 surface air is neutralized on average). The shift from  $PM_1$  to  $PM_{1.4}$  nitrate is consistent with the uptake of  
163  $HNO_3$  by coarse PM, with some of this uptake by dust coarser than 4  $\mu m$ . Half of the model overestimate of  
164  $HNO_3$  is corrected (Fig. 4e), with the remainder possibly due to an underestimate of  $HNO_3$  deposition  
165 velocity (Travis et al., 2022). The model overestimates nighttime nitrate in surface air at the KIST site,  
166 even with anthropogenic coarse PM. This nighttime nitrate in the model is driven by heterogeneous  $NO_2$   
167 and  $N_2O_5$  chemistry under stratified conditions, which could be subject to large local errors (Travis et al.,  
168 2022).



169 We also examined the effect of anthropogenic coarse PM on PM<sub>2.5</sub> nitrate concentrations in the NCP.  
170 Previous evaluation of GEOS-Chem with 2013 and 2015 PM<sub>2.5</sub> nitrate observations across China in  
171 summer and winter found no significant bias in 2015 or winter 2013 but an overestimate in summer 2013  
172 (Zhai et al., 2021a). That simulation did not include HNO<sub>3</sub> uptake by dust (natural or anthropogenic). We  
173 find here that including HNO<sub>3</sub> uptake by fine (PM<sub>2.5</sub>) dust has little effect on total PM<sub>2.5</sub> nitrate but  
174 partitions 10% of ammonium nitrate mass to fine dust nitrate in winter and 30% in summer (Fig. S4).  
175 Adding anthropogenic coarse PM in GEOS-Chem decreases modeled PM<sub>2.5</sub> nitrate in the NCP by 15% in  
176 winter and by 25% in summer, a relatively more modest effect than over the SMA because of larger excess  
177 of NH<sub>3</sub>.

#### 178 4. Implications for long-term trends of PM<sub>2.5</sub> nitrate and responses to emission controls

179 There are to our knowledge no continuous long-term records of PM<sub>2.5</sub> nitrate concentrations in China or  
180 South Korea. Figure 5 shows a multi-year compilation of winter and summer mean PM<sub>1</sub> and PM<sub>2.5</sub> nitrate  
181 observations from individual field campaigns in Beijing and Seoul over 2015-2021 (Table S1). We find no  
182 significant trends in winter, consistent with previous studies in the NCP that examined shorter periods (Fu  
183 et al., 2020). In summer, observations tend to show a decrease over the period but with large interannual  
184 variations driven by meteorology (Li et al., 2018; Zhai et al., 2021a).

185 Changes in anthropogenic emissions of NO<sub>x</sub>, SO<sub>2</sub>, NH<sub>3</sub>, PM<sub>2.5</sub>, and coarse PM could all affect PM<sub>2.5</sub>  
186 nitrate, and we used GEOS-Chem to investigate these effects for the 2015-2019 period. The Multi-  
187 resolution Emission Inventory for China (MEIC) reports that NO<sub>x</sub> emissions in the NCP decreased by 11%  
188 from 2015 to 2019, SO<sub>2</sub> emissions decreased by 54%, and primary PM<sub>2.5</sub> from combustion decreased by  
189 35% (Zheng et al., 2021a). This primary PM<sub>2.5</sub> includes a 40% contribution from mineral ash that we treat  
190 as anthropogenic fine dust and decreased by 27% from 2015 to 2019. The MEIC also reports a 15%  
191 decrease of NH<sub>3</sub> emissions over China from 2015 to 2019 (19% for the NCP), while the PKU-NH<sub>3</sub>  
192 emission inventory reports a 6% decrease over China from 2015 to 2018 (Liao et al., 2022). Observations  
193 of surface NO<sub>2</sub> and SO<sub>2</sub> over the SMA imply a 22% decrease of NO<sub>x</sub> emissions and a 40% decrease of SO<sub>2</sub>  
194 emissions during 2015-2019 (Bae et al., 2021; Colombi et al., 2022). Coarse PM decreased by 33% over  
195 the NCP and by 31% over SMA averaged for winter and summer.

196 Figure 6 shows the emission-driven changes of PM<sub>2.5</sub> nitrate over the NCP and SMA between 2015 and  
197 2019 as simulated by GEOS-Chem in sensitivity simulations applying emission trends for individual  
198 species (both in China and South Korea) to the same meteorological year (2019), with and without  
199 anthropogenic coarse PM. Sensitivities to emissions are qualitatively similar in both regions. Sensitivities  
200 to NH<sub>3</sub> and primary PM<sub>2.5</sub> emissions in the SMA are solely driven by emission trends in China since we  
201 assume no trends in South Korea for lack of better information.



202 The model reproduces the lack of trend in winter and the decreasing trend in summer seen in the  
203 observations for both the NCP and SMA. The lack of trend in winter reflects offsetting influences from  
204 decreasing  $\text{NO}_x$ ,  $\text{NH}_3$ , and primary  $\text{PM}_{2.5}$  emissions on the one hand, and decreasing  $\text{SO}_2$  and coarse PM  
205 emissions on the other hand. Decreasing  $\text{SO}_2$  increases the availability of  $\text{NH}_3$  for nitrate formation (Fu et  
206 al., 2020; Zhai et al., 2021a). Decreasing primary  $\text{PM}_{2.5}$  decreases fine dust nitrate and reduces the aerosol  
207 volume available for heterogeneous conversion of  $\text{NO}_x$  to nitrate (Shah et al., 2020b). Decreasing coarse  
208 PM has relatively little direct effect on  $\text{PM}_{2.5}$  nitrate in winter in the NCP because abundant atmospheric  
209  $\text{NH}_3$  combined with low temperatures and fast mass transfer drives  $\text{HNO}_3$  near-quantitatively to ammonium-  
210 nitrate particles, but it increases the sensitivity of  $\text{PM}_{2.5}$  nitrate to  $\text{NH}_3$  and  $\text{SO}_2$  emissions respectively by  
211 30% and 46% by providing an additional sink for the small fraction of  $\text{HNO}_3$  that remains in the gas phase  
212 and thus affecting the lifetime of total nitrate against dry deposition (Zhai et al., 2021a).

213 In summer, we find that the decrease in coarse PM over the 2015-2019 period directly cancels half of the  
214 benefit from decreasing  $\text{NO}_x$ ,  $\text{SO}_2$ ,  $\text{NH}_3$ , and primary  $\text{PM}_{2.5}$  emissions in the NCP, with less effect in the  
215 SMA. Unlike in winter, decreasing  $\text{SO}_2$  suppresses nitrate formation by decreasing the aerosol liquid water  
216 content (Stelson and Seinfeld, 1982). The effect of decreasing coarse PM emissions in summer is larger  
217 than in winter because warmer temperatures allow more  $\text{HNO}_3$  to remain in the gas phase under  $\text{NH}_3$ -  
218  $\text{HNO}_3$ - $\text{H}_2\text{SO}_4$  thermodynamics and thus be scavenged by coarse PM.

## 219 5. Conclusions

220 Coarse PM ( $\text{PM}_{10} - \text{PM}_{2.5}$ ) in urban areas of China and South Korea is very high year-round and is mainly  
221 of anthropogenic origin as fugitive dust except for natural desert dust events in spring. Annual mean coarse  
222 PM concentrations decreased by 21% from 2015 to 2019 in both the North China Plain (NCP) and the  
223 Seoul Metropolitan Area (SMA), with steeper decreases in 2020 because of COVID-19 restrictions on  
224 traffic and construction.

225 Anthropogenic coarse PM is of direct air quality concern in accounting for about half of  $\text{PM}_{10}$  in the  
226 NCP and the SMA, but it also takes up  $\text{HNO}_3$  effectively and can thus suppress formation of fine  
227 particulate nitrate which is a major component of  $\text{PM}_{2.5}$  pollution. Comparison of GEOS-Chem model  
228 simulations to surface and aircraft observations from the KORUS-AQ campaign over the SMA in May-  
229 June 2016 shows that accounting for anthropogenic coarse PM largely corrects previous model  
230 overestimates of fine particulate nitrate.

231 Decrease in anthropogenic coarse PM emissions to improve  $\text{PM}_{10}$  air quality could have unintended  
232 consequence of increasing  $\text{PM}_{2.5}$  nitrate, offsetting the gains from decreases in  $\text{NO}_x$  and  $\text{NH}_3$  emissions.  
233 Compilation of 2015-2021 observations of fine particulate nitrate in Beijing and Seoul suggests little trend  
234 in winter and a decrease in summer, consistent with GEOS-Chem. Decreasing coarse PM in the model in



235 winter increases PM<sub>2.5</sub> nitrate both directly and indirectly by increasing the sensitivity to decreases in SO<sub>2</sub>  
236 emissions. In summer, decreasing coarse PM offsets half of the PM<sub>2.5</sub> nitrate decrease in the NCP that  
237 would be expected from decreases in NO<sub>x</sub>, SO<sub>2</sub>, and NH<sub>3</sub> emissions. As coarse PM continues to decrease in  
238 response to fugitive dust pollution control, there is a greater need to reduce NH<sub>3</sub> and NO<sub>x</sub> emissions in  
239 order to decrease fine particulate nitrate air pollution in East Asia.

240

241 *Data availability.* PM<sub>2.5</sub>, PM<sub>10</sub>, and CO data over China are from <http://www.quotsoft.net/air/>, over South  
242 Korea are from [https://www.airkorea.or.kr/web/last\\_amb\\_hour\\_data?pMENU\\_NO=123](https://www.airkorea.or.kr/web/last_amb_hour_data?pMENU_NO=123). Surface and  
243 aircraft data during KORUS-AQ are from <https://doi.org/10.5067/Suborbital/KORUSAQ/DATA01>. Multi-  
244 year compilation of winter and summer mean PM<sub>1</sub> and PM<sub>2.5</sub> nitrate are provided in Table S1.

245

246 *Supplement.* The supplement related to this article is uploaded at submission.

247

248 *Author Contributions.* S.Z. and D.J.J. designed the research. S.Z. performed the research. D.C.P., N.K.C.,  
249 V.S., L.H.Y., and H.L. helped with data analysis and results interpretation. Q.Z. provided the MEIC  
250 emission inventory. S.W., H.K., Y.S., J.S.C, J.S.P., J.E.D., T.L., J.S.H, and B.E.A provided observation  
251 data. J.H.W. and Y.K. provided the KORUSv5 emission inventory. G.L., F.Y., and K.L. helped with model  
252 simulations. S.Z. and D.J.J wrote the paper with input from all other authors.

253

254 *Competing Interests.* The authors declare no competing interests.

255

256 *Financial support.* This work was funded by the Harvard–NUIST Joint Laboratory for Air Quality and  
257 Climate (JLAQC) and the Samsung Advanced Institute of Technology.

258

259 *Acknowledgments.* We thank Bo Zheng (Tsinghua Shenzhen International Graduate School, Tsinghua  
260 University) for processing the MEIC emission inventory. We thank Paul O. Wennberg, Michelle J. Kim,  
261 Alexander P. Teng, and John D. Crouse from the California Institute of Technology for their contributions  
262 to HNO<sub>3</sub> measurements during KORUS-AQ.

263

## 264 **References**

- 265 Bae, M., Kim, B.-U., Kim, H. C., Kim, J., and Kim, S.: Role of emissions and meteorology in the recent  
266 PM<sub>2.5</sub> changes in China and South Korea from 2015 to 2018, *Environ. Pollut.*, 270, 116233,  
267 <https://doi.org/10.1016/j.envpol.2020.116233>, 2021.
- 268 Chen, R., Yin, P., Meng, X., Wang, L., Liu, C., Niu, Y., Liu, Y., Liu, J., Qi, J., You, J., Kan, H., and Zhou,  
269 M.: Associations between Coarse Particulate Matter Air Pollution and Cause-Specific Mortality: A  
270 Nationwide Analysis in 272 Chinese Cities, *Environ. Health Perspect.*, 127, 017008,  
271 <https://doi.org/10.1289/EHP2711>, 2019.



- 272 Colombi, N. K., Jacob, D. J., Yang, L. H., Zhai, S., Shah, V., Grange, S. K., Yantosca, R. M., Kim, S., and  
273 Liao, H.: Why is ozone in South Korea and the Seoul Metropolitan Area so high and increasing?,  
274 EGU sphere, 2022, 1-21, <https://doi.org/10.5194/egusphere-2022-1366>, 2022.
- 275 Chinese State Council: Action Plan on Prevention and Control of Air Pollution, Chinese State Council,  
276 [http://www.gov.cn/zwgc/2013-09/12/content\\_2486773.htm](http://www.gov.cn/zwgc/2013-09/12/content_2486773.htm) (last access: December 18 2022), 2013 (in  
277 Chinese).
- 278 Chinese State Council: Three-year Action Plan for Protecting Blue Sky, Chinese State Council,  
279 [http://www.gov.cn/zhengce/content/2018-07/03/content\\_5303158.htm](http://www.gov.cn/zhengce/content/2018-07/03/content_5303158.htm) (last access: December 18  
280 2022), 2018 (in Chinese).
- 281 Chinese State Council: Beijing has set up more than 1,000 sites to monitor dust, Chinese State Council,  
282 [http://www.gov.cn/xinwen/2019-04/16/content\\_5383488.htm](http://www.gov.cn/xinwen/2019-04/16/content_5383488.htm) (last access: December 18 2022), 2019  
283 (in Chinese).
- 284 Crawford, J. H., Ahn, J.-Y., Al-Saadi, J., Chang, L., Emmons, L. K., Kim, J., Lee, G., Park, J.-H., Park, R.  
285 J., Woo, J. H., Song, C.-K., Hong, J.-H., Hong, Y.-D., Lefer, B. L., Lee, M., Lee, T., Kim, S., Min, K.-  
286 E., Yum, S. S., Shin, H. J., Kim, Y.-W., Choi, J.-S., Park, J.-S., Szykman, J. J., Long, R. W., Jordan,  
287 C. E., Simpson, I. J., Fried, A., Dibb, J. E., Cho, S., and Kim, Y. P.: The Korea–United States Air  
288 Quality (KORUS-AQ) field study, *Elementa-Sci. Anthropol.*, 9 (1), 1-27,  
289 <https://doi.org/10.1525/elementa.2020.00163>, 2021.
- 290 Dibb, J. E., Talbot, R. W., Scheuer, E. M., Seid, G., Avery, M. A., and Singh, H. B.: Aerosol chemical  
291 composition in Asian continental outflow during the TRACE-P campaign: Comparison with PEM-  
292 West B, *J. Geophys. Res. Atmos.*, 108, 8815, <https://doi.org/10.1029/2002JD003111>, 2003.
- 293 Fairlie, T. D., Jacob, D. J., Dibb, J. E., Alexander, B., Avery, M. A., van Donkelaar, A., and Zhang, L.:  
294 Impact of mineral dust on nitrate, sulfate, and ozone in transpacific Asian pollution plumes, *Atmos.*  
295 *Chem. Phys.*, 10, 3999-4012, <https://doi.org/10.5194/acp-10-3999-2010>, 2010.
- 296 Fu, X., Wang, T., Gao, J., Wang, P., Liu, Y., Wang, S., Zhao, B., and Xue, L.: Persistent Heavy Winter  
297 Nitrate Pollution Driven by Increased Photochemical Oxidants in Northern China, *Environ. Sci.*  
298 *Technol.*, 54, 3881–3889, <https://doi.org/10.1021/acs.est.9b07248>, 2020.
- 299 Heim, E. W., Dibb, J., Scheuer, E., Jost, P. C., Nault, B. A., Jimenez, J. L., Peterson, D., Knote, C., Fenn,  
300 M., Hair, J., Beyersdorf, A. J., Corr, C., and Anderson, B. E.: Asian dust observed during KORUS-AQ  
301 facilitates the uptake and incorporation of soluble pollutants during transport to South Korea, *Atmos.*  
302 *Environ.*, 224, 117305, <https://doi.org/10.1016/j.atmosenv.2020.117305>, 2020.
- 303 Hodzic, A., Bessagnet, B., and Vautard, R.: A model evaluation of coarse-mode nitrate heterogeneous  
304 formation on dust particles, *Atmos. Environ.*, 40, 4158-4171,  
305 <https://doi.org/10.1016/j.atmosenv.2006.02.015>, 2006.
- 306 Huynh, H. N. and McNeill, V. F.: Heterogeneous Chemistry of CaCO<sub>3</sub> Aerosols with HNO<sub>3</sub> and HCl, *J.*  
307 *Phys. Chem.*, 124, 3886-3895, <https://doi.org/10.1021/acs.jpca.9b11691>, 2020.
- 308 Jeong, J. I., Seo, J., and Park, R. J.: Compromised Improvement of Poor Visibility Due to PM Chemical  
309 Composition Changes in South Korea, *Remote Sens.*, 14, 5310, <https://doi.org/10.3390/rs14215310>,  
310 2022.
- 311 Kakavas, S. and Pandis, S. N.: Effects of urban dust emissions on fine and coarse PM levels and  
312 composition, *Atmos. Environ.*, 246, 118006, <https://doi.org/10.1016/j.atmosenv.2020.118006>, 2021.
- 313 Katra, I.: Soil Erosion by Wind and Dust Emission in Semi-Arid Soils Due to Agricultural Activities,  
314 *Agronomy*, 10 (1), 89, <https://doi.org/10.3390/agronomy10010089>, 2020.
- 315 Kim, H., Zhang, Q., and Heo, J.: Influence of intense secondary aerosol formation and long-range transport  
316 on aerosol chemistry and properties in the Seoul Metropolitan Area during spring time: results from  
317 KORUS-AQ, *Atmos. Chem. Phys.*, 18, 7149-7168, <https://doi.org/10.5194/acp-18-7149-2018>, 2018.



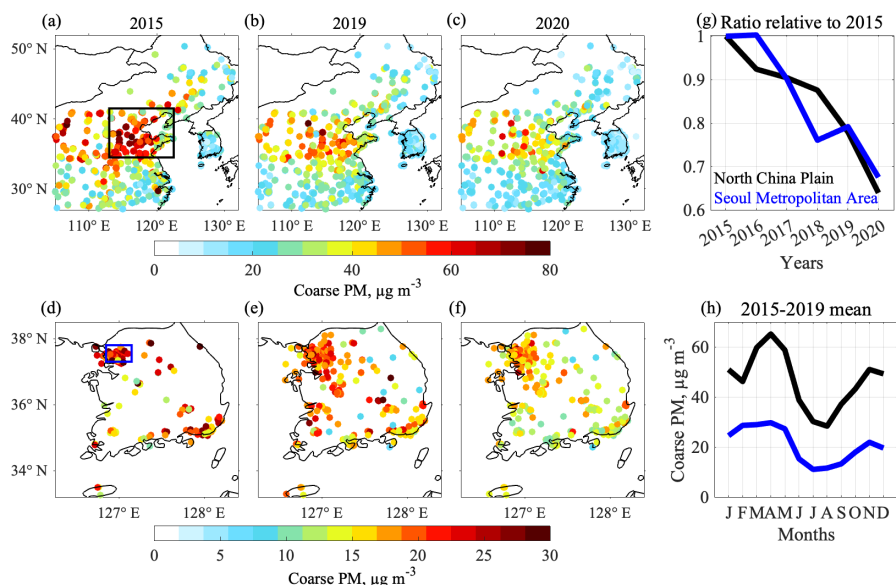
- 318 Kim, H., Zhang, Q., and Sun, Y.: Measurement report: Characterization of severe spring haze episodes and  
319 influences of long-range transport in the Seoul metropolitan area in March 2019, *Atmos. Chem. Phys.*,  
320 20, 11527-11550, <https://doi.org/10.5194/acp-20-11527-2020>, 2020.
- 321 Kim, H., Zhang, Q., Bae, G. N., Kim, J. Y., and Lee, S. B.: Sources and atmospheric processing of winter  
322 aerosols in Seoul, Korea: insights from real-time measurements using a high-resolution aerosol mass  
323 spectrometer, *Atmos. Chem. Phys.*, 17, 2009-2033, <https://doi.org/10.5194/acp-17-2009-2017>, 2017.
- 324 Lee, H., Honda, Y., Hashizume, M., Guo, Y. L., Wu, C.-F., Kan, H., Jung, K., Lim, Y.-H., Yi, S., and Kim,  
325 H.: Short-term exposure to fine and coarse particles and mortality: A multicity time-series study in  
326 East Asia, *Environ. Pollut.*, 207, 43-51, <https://doi.org/10.1016/j.envpol.2015.08.036>, 2015.
- 327 Li, H., Cheng, J., Zhang, Q., Zheng, B., Zhang, Y., Zheng, G., and He, K.: Rapid transition in winter  
328 aerosol composition in Beijing from 2014 to 2017: response to clean air actions, *Atmos. Chem. Phys.*,  
329 19, 11485-11499, <https://doi.org/10.5194/acp-19-11485-2019>, 2019.
- 330 Li, H., Zhang, Q., Zheng, B., Chen, C., Wu, N., Guo, H., Zhang, Y., Zheng, Y., Li, X., and He, K.: Nitrate-  
331 driven urban haze pollution during summertime over the North China Plain, *Atmos. Chem. Phys.*, 18,  
332 5293-5306, <https://doi.org/10.5194/acp-18-5293-2018>, 2018.
- 333 Li, T., Bi, X., Dai, Q., Wu, J., Zhang, Y., and Feng, Y.: Optimized approach for developing soil fugitive  
334 dust emission inventory in "2+26" Chinese cities, *Environ. Pollut.*, 285, 117521,  
335 <https://doi.org/10.1016/j.envpol.2021.117521>, 2021a.
- 336 Li, T., Dong, W., Dai, Q., Feng, Y., Bi, X., Zhang, Y., and Wu, J.: Application and validation of the  
337 fugitive dust source emission inventory compilation method in Xiong'an New Area, China, *Sci. Total*  
338 *Environ.*, 798, 149114, <https://doi.org/10.1016/j.scitotenv.2021.149114>, 2021b.
- 339 Li, T., Ma, S., Liang, W., Li, L., Dai, Q., Bi, X., Wu, J., Zhang, Y., and Feng, Y.: Application of the high  
340 spatiotemporal resolution soil fugitive dust emission inventory compilation method based on CAMx  
341 model, *Atmos. Res.*, 262, 105770, <https://doi.org/10.1016/j.atmosres.2021.105770>, 2021c.
- 342 Liao, W., Liu, M., Huang, X., Wang, T., Xu, Z., Shang, F., Song, Y., Cai, X., Zhang, H., Kang, L., and  
343 Zhu, T.: Estimation for ammonia emissions at county level in China from 2013 to 2018, *Sci. China*  
344 *Earth Sci.*, 65, 1116-1127, <https://doi.org/10.1007/s11430-021-9897-3>, 2022.
- 345 Liu, H., Jacob, D. J., Bey, I., and Yantosca, R. M.: Constraints from  $^{210}\text{Pb}$  and  $^7\text{Be}$  on wet deposition and  
346 transport in a global three-dimensional chemical tracer model driven by assimilated meteorological  
347 fields, *J. Geophys. Res. Atmos.*, 106, 12109-12128, <https://doi.org/10.1029/2000JD900839>, 2001.
- 348 Liu, S., Xing, J., Sahu, S. K., Liu, X., Liu, S., Jiang, Y., Zhang, H., Li, S., Ding, D., Chang, X., and Wang,  
349 S.: Wind-blown dust and its impacts on particulate matter pollution in Northern China: current and  
350 future scenarios, *Environ. Res. Lett.*, 16, 114041, <http://dx.doi.org/10.1088/1748-9326/ac31ec>, 2021.
- 351 Liu, Y., Gibson, C., Wang, H., Grassian, and Laskin, A.: Kinetics of Heterogeneous Reaction of  $\text{CaCO}_3$   
352 particles with Gaseous  $\text{HNO}_3$  over a Wide Range of Humidity, *J. Phys. Chem. A*, 112, 1561-1571,  
353 <https://doi.org/10.1021/jp076169h>, 2008.
- 354 Luo, G., Yu, F., and Schwab, J.: Revised treatment of wet scavenging processes dramatically improves  
355 GEOS-Chem 12.0.0 simulations of nitric acid, nitrate, and ammonium over the United States, *Geosci.*  
356 *Model Dev.*, 12, 3439-3447 <https://doi.org/10.5194/gmd-12-3439-2019>, 2019.
- 357 McNaughton, C. S., Clarke, A. D., Howell, S. G., Pinkerton, M., Anderson, B., Thornhill, L., Hudgins, C.,  
358 Winstead, E., Dibb, J. E., Scheuer, E., and Maring, H.: Results from the DC-8 Inlet Characterization  
359 Experiment (DICE): Airborne Versus Surface Sampling of Mineral Dust and Sea Salt Aerosols,  
360 *Aerosol Sci. Tech.*, 41, 136-159, <https://doi.org/10.1080/02786820601118406>, 2007.
- 361 Mgelwa, A. S., Song, L., Fan, M., Li, Z., Zhang, Y., Chang, Y., Pan, Y., Gurmesa, G. A., Liu, D., Huang,  
362 S., Qiu, Q., and Fang, Y.: Isotopic imprints of aerosol ammonium over the north China plain, *Environ.*  
363 *Pollut.*, 315, 120376, <https://doi.org/10.1016/j.envpol.2022.120376>, 2022.



- 364 Noh, H.-j., Lee, S.-k., and Yu, J.-h.: Identifying Effective Fugitive Dust Control Measures for Construction  
365 Projects in Korea, *Sustainability*, 10, 1206, <https://doi.org/10.3390/su10041206>, 2018.
- 366 Park, S. H., Song, C. B., Kim, M. C., Kwon, S. B., and Lee, K. W.: Study on Size Distribution of Total  
367 Aerosol and Water-Soluble Ions During an Asian Dust Storm Event at Jeju Island, Korea, *Environ.*  
368 *Monit. Assess.*, 93, 157-183, <https://doi.org/10.1023/B:EMAS.0000016805.04194.56>, 2004.
- 369 Park, R. J., Oak, Y. J., Emmons, L. K., Kim, C.-H., Pfister, G. G., Carmichael, G. R., Saide, P. E., Cho, S.-  
370 Y., Kim, S., Woo, J.-H., Crawford, J. H., Gaubert, B., Lee, H.-J., Park, S.-Y., Jo, Y.-J., Gao, M., Tang,  
371 B., Stanier, C. O., Shin, S. S., Park, H. Y., Bae, C., and Kim, E.: Multi-model intercomparisons of air  
372 quality simulations for the KORUS-AQ campaign, *Elementa-Sci. Anthropol.*, 9, 00139,  
373 <https://doi.org/10.1525/elementa.2021.00139>, 2021.
- 374 Philip, S., Martin, R. V., Snider, G., Weagle, C. L., van Donkelaar, A., Brauer, M., Henze, D. K., Klimont,  
375 Z., Venkataraman, C., and Guttikunda, S. K.: Anthropogenic fugitive, combustion and industrial dust  
376 is a significant, underrepresented fine particulate matter source in global atmospheric models, *Environ.*  
377 *Res. Lett.*, 12, 044018, <https://doi.org/10.1088/1748-9326/aa65a4>, 2017.
- 378 Qiu, H., Tian, L. W., Pun, V. C., Ho, K.-f., Wong, T. W., and Yu, I. T. S.: Coarse particulate matter  
379 associated with increased risk of emergency hospital admissions for pneumonia in Hong Kong,  
380 *Respiratory Epidemiology*, 69, 1027, <http://dx.doi.org/10.1136/thoraxjnl-2014-205429>, 2014.
- 381 Shah, V., Jacob, D. J., Moch, J. M., Wang, X., and Zhai, S.: Global modeling of cloud water acidity,  
382 precipitation acidity, and acid inputs to ecosystems, *Atmos. Chem. Phys.*, 20, 12223-12245,  
383 <https://doi.org/10.5194/acp-20-12223-2020>, 2020a.
- 384 Shah, V., Jacob, D. J., Li, K., Silvern, R. F., Zhai, S., Liu, M., Lin, J., and Zhang, Q.: Effect of changing  
385 NO<sub>x</sub> lifetime on the seasonality and long-term trends of satellite-observed tropospheric NO<sub>2</sub> columns  
386 over China, *Atmos. Chem. Phys.*, 20, 1483-1495, <https://doi.org/10.5194/acp-20-1483-2020>, 2020b.
- 387 Shao, Y. and Dong, C. H.: A review on East Asian dust storm climate, modelling and monitoring, *Glob.*  
388 *Planet. Change*, 52, 1-22, <https://doi.org/10.1016/j.gloplacha.2006.02.011>, 2006.
- 389 Stelson, A. W. and Seinfeld, J. H.: Thermodynamic prediction of the water activity, NH<sub>4</sub>NO<sub>3</sub> dissociation  
390 constant, density and refractive index for the NH<sub>4</sub>NO<sub>3</sub>-(NH<sub>4</sub>)<sub>2</sub>SO<sub>4</sub>-H<sub>2</sub>O system at 25° C, *Atmos.*  
391 *Environ.*, 16, 2507-2514, [https://doi.org/10.1016/0004-6981\(82\)90142-1](https://doi.org/10.1016/0004-6981(82)90142-1), 1982.
- 392 Stone, E. A., Yoon, S.-C., and Schauer, J. J.: Chemical Characterization of Fine and Coarse Particles in  
393 Gosan, Korea during Springtime Dust Events, *Aerosol Air Qual. Res.*, 11, 31-43,  
394 <http://dx.doi.org/10.4209/aaqr.2010.08.0069>, 2011.
- 395 Tang, Y. and Han, G.: Characteristics of major elements and heavy metals in atmospheric dust in Beijing,  
396 China, *J. Geochem. Explor.*, 176, 114-119, <https://doi.org/10.1016/j.gexplo.2015.12.002>, 2017.
- 397 Tian, R., Ma, X., Sha, T., Pan, X., and Wang, Z.: Exploring dust heterogeneous chemistry over China:  
398 Insights from field observation and GEOS-Chem simulation, *Sci. Total Environ.*, 798, 149307,  
399 <https://doi.org/10.1016/j.scitotenv.2021.149307>, 2021.
- 400 Travis, K. R., Crawford, J. H., Chen, G., Jordan, C. E., Nault, B. A., Kim, H., Jimenez, J. L., Campuzano-  
401 Jost, P., Dibb, J. E., Woo, J. H., Kim, Y., Zhai, S., Wang, X., McDuffie, E. E., Luo, G., Yu, F., Kim,  
402 S., Simpson, I. J., Blake, D. R., Chang, L., and Kim, M. J.: Limitations in representation of physical  
403 processes prevent successful simulation of PM<sub>2.5</sub> during KORUS-AQ, *Atmos. Chem. Phys.*, 22,  
404 7933-7958, <https://doi.org/10.5194/acp-22-7933-2022>, 2022.
- 405 Wang, X., Zhang, L., Yao, Z., Ai, S., Qian, Z., Wang, H., BeLue, R., Liu, T., Xiao, J., Li, X., Zeng, W.,  
406 Ma, W., and Lin, H.: Ambient coarse particulate pollution and mortality in three Chinese cities:  
407 Association and attributable mortality burden, *Sci. Total Environ.*, 628-629, 1037-1042,  
408 <https://doi.org/10.1016/j.scitotenv.2018.02.100>, 2018a.

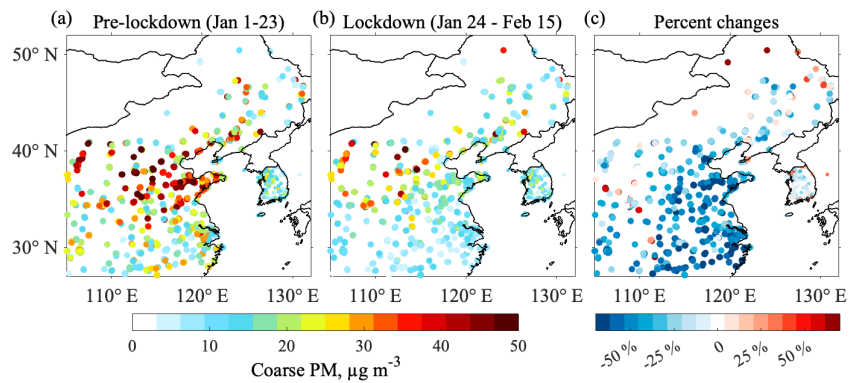


- 409 Wang, Z., Pan, X., Uno, I., Chen, X., Yamamoto, S., Zheng, H., Li, J., and Wang, Z.: Importance of  
410 mineral dust and anthropogenic pollutants mixing during a long-lasting high PM event over East Asia,  
411 *Environ. Pollut.*, 234, 368-378, <https://doi.org/10.1016/j.envpol.2017.11.068>, 2018b.
- 412 Wang, Z., Pan, X., Uno, I., Li, J., Wang, Z., Chen, X., Fu, P., Yang, T., Kobayashi, H., Shimizu, A.,  
413 Sugimoto, N., and Yamamoto, S.: Significant impacts of heterogeneous reactions on the chemical  
414 composition and mixing state of dust particles: A case study during dust events over northern China,  
415 *Atmos. Environ.*, 159, 83-91, <https://doi.org/10.1016/j.atmosenv.2017.03.044>, 2017.
- 416 Wesely, M. L.: Parameterization of surface resistances to gaseous dry deposition in regional-scale  
417 numerical models, *Atmos. Environ.*, 23, 1293-1304, [https://doi.org/10.1016/0004-6981\(89\)90153-4](https://doi.org/10.1016/0004-6981(89)90153-4),  
418 1989.
- 419 Woo, J.-H., Kim, Y., Kim, H.-K., Choi, K.-C., Eum, J.-H., Lee, J.-B., Lim, J.-H., Kim, J., and Seong, M.:  
420 Development of the CREATE Inventory in Support of Integrated Climate and Air Quality Modeling  
421 for Asia, *Sustainability*, 12, 7930, <https://doi.org/10.3390/su12197930>, 2020.
- 422 Wu, Z., Zhang, X., and Wu, M.: Mitigating construction dust pollution: state of the art and the way  
423 forward, *J. Clean. Prod.*, 112, 1658-1666, <https://doi.org/10.1016/j.jclepro.2015.01.015>, 2016.
- 424 Xing, J., Ye, K., Zuo, J., and Jiang, W.: Control Dust Pollution on Construction Sites: What Governments  
425 Do in China?, *Sustainability*, 10, 2945, <https://doi.org/10.3390/su10082945>, 2018.
- 426 Xu, Q., Wang, S., Jiang, J., Bhattarai, N., Li, X., Chang, X., Qiu, X., Zheng, M., Hua, Y., and Hao, J.:  
427 Nitrate dominates the chemical composition of PM<sub>2.5</sub> during haze event in Beijing, China, *Sci. Total  
428 Environ.*, 689, 1293-1303, <https://doi.org/10.1016/j.scitotenv.2019.06.294>, 2019.
- 429 Zhai, S., Jacob, D. J., Wang, X., Liu, Z., Wen, T., Shah, V., Li, K., Moch, J. M., Bates, K. H., Song, S.,  
430 Shen, L., Zhang, Y., Luo, G., Yu, F., Sun, Y., Wang, L., Qi, M., Tao, J., Gui, K., Xu, H., Zhang, Q.,  
431 Zhao, T., Wang, Y., Lee, H. C., Choi, H., and Liao, H.: Control of particulate nitrate air pollution in  
432 China, *Nat. Geosci.*, 14, 389-395, <https://doi.org/10.1038/s41561-021-00726-z>, 2021a.
- 433 Zhai, S., Jacob, D. J., Brewer, J. F., Li, K., Moch, J. M., Kim, J., Lee, S., Lim, H., Lee, H. C., Kuk, S. K.,  
434 Park, R. J., Jeong, J. I., Wang, X., Liu, P., Luo, G., Yu, F., Meng, J., Martin, R. V., Travis, K. R., Hair,  
435 J. W., Anderson, B. E., Dibb, J. E., Jimenez, J. L., Campuzano-Jost, P., Nault, B. A., Woo, J. H., Kim,  
436 Y., Zhang, Q., and Liao, H.: Relating geostationary satellite measurements of aerosol optical depth  
437 (AOD) over East Asia to fine particulate matter (PM<sub>2.5</sub>): insights from the KORUS-AQ aircraft  
438 campaign and GEOS-Chem model simulations, *Atmos. Chem. Phys.*, 21, 16775-16791,  
439 <https://doi.org/10.5194/acp-21-16775-2021>, 2021b.
- 440 Zhang, Q., Shen, Z., Cao, J., Ho, K., Zhang, R., Bie, Z., Chang, H., and Liu, S.: Chemical profiles of urban  
441 fugitive dust over Xi'an in the south margin of the Loess Plateau, China, *Atmos. Pollut. Res.*, 5, 421-  
442 430, <https://doi.org/10.5094/APR.2014.049>, 2014.
- 443 Zhao, G., Chen, Y., Hopke, P. K., Holsen, T. M., and Dhaniyala, S.: Characteristics of traffic-induced  
444 fugitive dust from unpaved roads, *Aerosol Sci. Technol.*, 51, 1324-1331,  
445 <https://doi.org/10.1080/02786826.2017.1347251>, 2017.
- 446 Zheng, B., Zhang, Q., Geng, G., Chen, C., Shi, Q., Cui, M., Lei, Y., and He, K.: Changes in China's  
447 anthropogenic emissions and air quality during the COVID-19 pandemic in 2020, *Earth Syst. Sci.  
448 Data*, 13, 2895-2907, <https://doi.org/10.5194/essd-13-2895-2021>, 2021a.
- 449 Zheng, B., Cheng, J., Geng, G., Wang, X., Li, M., Shi, Q., Qi, J., Lei, Y., Zhang, Q., and He, K.: Mapping  
450 anthropogenic emissions in China at 1 km spatial resolution and its application in air quality modeling,  
451 *Sci. Bull.*, 66, 612-620, <https://doi.org/10.1016/j.scib.2020.12.008>, 2021b.
- 452 Zheng, B., Tong, D., Li, M., Liu, F., Hong, C., Geng, G., Li, H., Li, X., Peng, L., Qi, J., Yan, L., Zhang, Y.,  
453 Zhao, H., Zheng, Y., He, K., and Zhang, Q.: Trends in China's anthropogenic emissions since 2010 as  
454 the consequence of clean air actions, *Atmos. Chem. Phys.*, 18, 14095-14111,  
455 <https://doi.org/10.5194/acp-18-14095-2018>, 2018.



456

457 **Figure 1.** Distributions and trends of coarse PM concentrations over China and South Korea during 2015-2020. Here  
 458 and elsewhere, coarse particulate matter (PM) is defined as particles between 2.5 and 10  $\mu\text{m}$  aerodynamic diameter and  
 459 its concentration is determined by subtracting  $\text{PM}_{2.5}$  from  $\text{PM}_{10}$  in the air quality network data. Panels (a)-(c) show the  
 460 annual mean concentrations in 2015, 2019, and 2020 over China and panels (d)-(f) show the same for South Korea. The  
 461 rectangles in (a) and (d) delineate the North China Plain or NCP (113 - 122.5° E, 34.5 - 41.5° N) and the Seoul  
 462 Metropolitan area or SMA (126.7 - 127.3° E, 37.3 - 37.8° N). Panel (g) shows annual trends relative to 2015 in the  
 463 NCP (197 sites) and the SMA (33 sites) averaged over sites with at least 70% data coverage each year from 2015 to  
 464 2020. Panel (h) shows the mean 2015-2019 seasonality over the NCP and SMA.  
 465

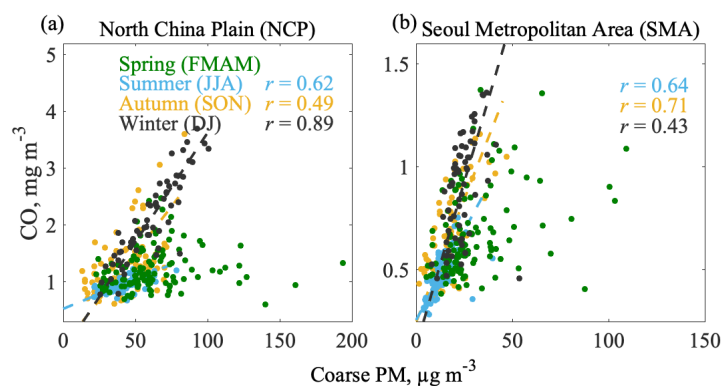


466

467 **Figure 2.** Response of coarse PM to COVID-19 lockdown in China. (a) Coarse PM averaged for the three weeks  
468 before the China national lockdown (January 1-23, 2020). (b) Coarse PM averaged during the three-week lockdown  
469 (January 24 - February 15, 2020). (c) Percent changes of coarse PM between lockdown and pre-lockdown periods.

470

471

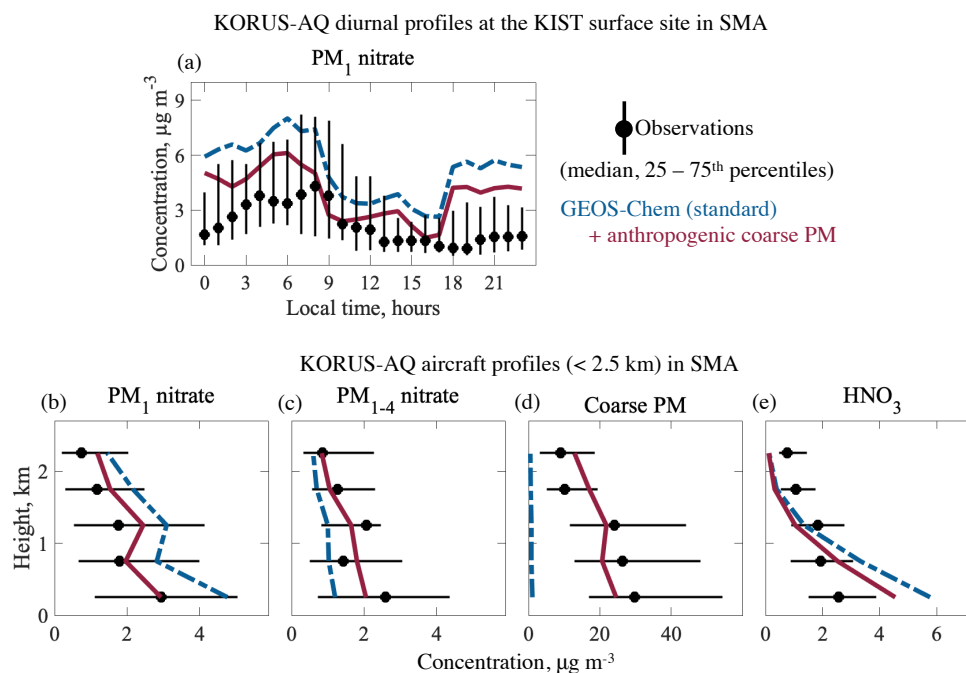


472

473 **Figure 3.** Daily correlations of coarse PM and CO concentrations over the North China Plain (NCP) and Seoul  
474 Metropolitan Area (SMA) in 2015. Coarse PM and CO concentrations are 24-h averages of air quality network  
475 observations spatially averaged over the two regions. Also shown are the correlation coefficients and reduced-major-  
476 axis regression lines except in spring when the correlation is not significant ( $p$ -value  $> 0.05$ ). We include February in  
477 spring to cover the season of natural dust events (Tang and Han, 2017).

478

479

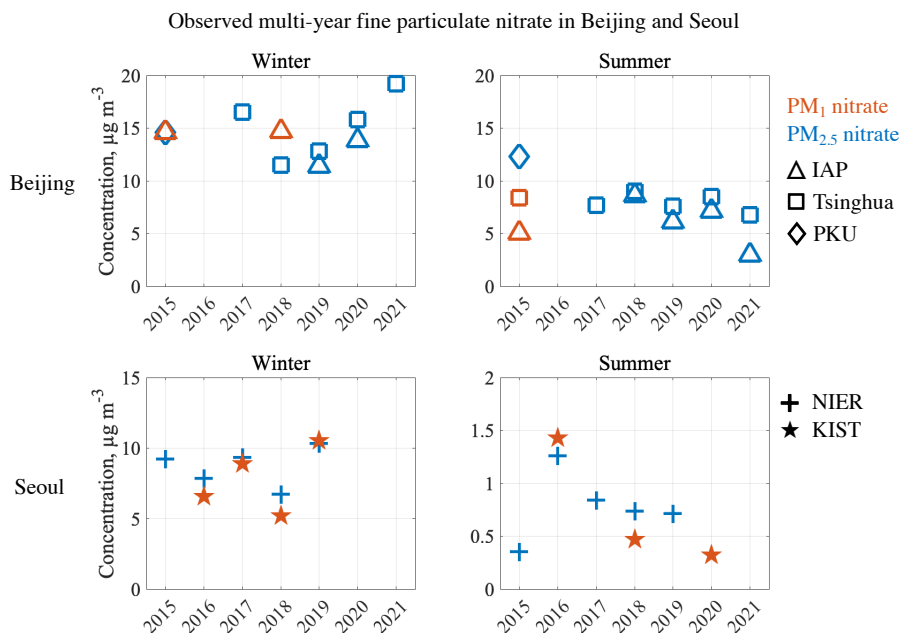


480

481 **Figure 4.** Effect of anthropogenic coarse PM on nitrate concentrations over the Seoul Metropolitan Area (SMA) during  
 482 the KORUS-AQ campaign (May–June 2016). GEOS-Chem model results without (standard) and with anthropogenic  
 483 coarse PM are compared to surface and aircraft observations. (a) Median diurnal variation (error bars are 25<sup>th</sup> and 75<sup>th</sup>  
 484 percentiles) of PM<sub>1</sub> nitrate at the Korea Institute of Science and Technology (KIST) site. (b)–(e) Median vertical  
 485 profiles of PM<sub>1</sub> nitrate, PM<sub>1-4</sub> nitrate, coarse PM (PM<sub>2.5-10</sub>), and HNO<sub>3</sub> concentrations for the ensemble of flights over  
 486 the SMA. Horizontal bars for the observations indicate 25<sup>th</sup>–75<sup>th</sup> percentiles.

487

488

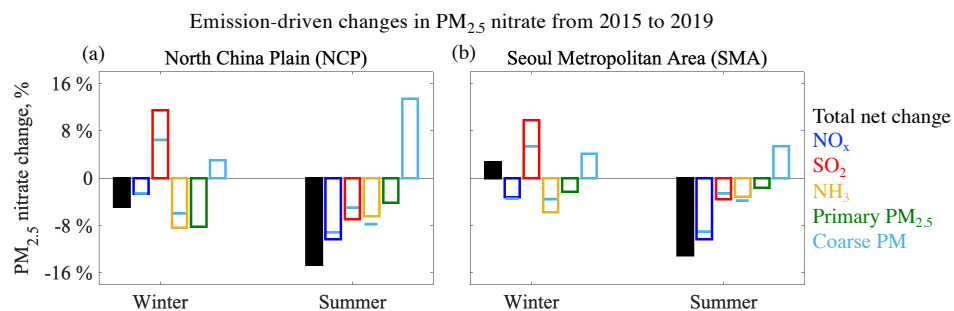


489

490 **Figure 5.** Long-term trend of fine particulate nitrate concentrations in Beijing and Seoul over the 2015-2021 period.  
 491 Mean PM<sub>1</sub> or PM<sub>2.5</sub> concentrations in winter and summer are compiled from individual field campaigns in Beijing at  
 492 the Institute of Atmospheric Physics (IAP), Tsinghua University (Tsinghua), and Peking University (PKU) sites and in  
 493 Seoul at the National Institute of Environmental Research (NIER) and Korea Institute of Science and Technology  
 494 (KIST) sites (Table S1). Note the differences in scales between panels.

495

496



Emission changes from 2015 to 2019

	NO <sub>x</sub>	SO <sub>2</sub>	NH <sub>3</sub>	Primary PM <sub>2.5</sub>	Coarse PM
NCP	-11%	-54%	-19%	-35%	-33%
SMA	-22%	-40%	0%	0%	-31%

497

498 **Figure 6.** Emission-driven changes in mean PM<sub>2.5</sub> nitrate from 2015 to 2019 over the NCP and SMA. Results are from  
 499 GEOS-Chem sensitivity simulations including total and individual emission changes over the period, all for the same  
 500 meteorological year (2019) and applied both to China and South Korea (so the effects of NH<sub>3</sub> and primary PM<sub>2.5</sub> over  
 501 the SMA are due to long-range transport from China). Values are seasonal means for winter and summer. The blue  
 502 lines superimposed on the NO<sub>x</sub>, SO<sub>2</sub>, and NH<sub>3</sub> sensitivity bars show the effects from simulations not accounting for the  
 503 effect of HNO<sub>3</sub> uptake by anthropogenic coarse PM.

504